RSC Advances

ROYAL SOCIETY OF CHEMISTRY

www.rsc.org/advances

Heteroatom-doped porous carbon derived from the "all-in-one" precursor sewage sludge for electrochemical energy storage†

Shi-Jie Yuan, Xiao-Hu Dai*

State Key Laboratory of Pollution Control and Resource Reuse, College of Environmental Science and Engineering, Tongji University, Shanghai, 200092, China

***Corresponding author:**

Prof. Xiao-Hu Dai, Phone: +86-21-65986297; Fax: +86-21-65983602; E-mail: daixiaohu@tongji.edu.cn

†Electronic supplementary information (ESI) available: Energy dispersive X-ray, FTIR and Raman spectra. See DOI: 10.1039/xxxxxxxxxx.

ABSTRACT

With the imposition of more stringent regulations governing the disposal and use of sewage sludge, the need to develop more cost-effective and environmentally benign re-uses of sewage sludge is of particular concern. Pyrolysis converting the sewage sludge to porous carbon is an emerging technology for the disposal of huge amounts of sewage sludge. In this study, a unique heteroatom-doped porous carbon was prepared via the direct pyrolysis of sewage sludge with SiO_2, transition metals and organic matter, the special components of sewage sludge, acted as the in-built template, the graphitizing catalysts, and the ideal precursor and nature dopant, respectively. The as-prepared N, O-doped porous carbon had a high specific surface area, numerous heteroatoms, good electrical transport properties and a meso-/macroporous composite. It exhibited favorable charge storage capacity and good stability over 10000 cycles. The supercapacitor performance results from its hierarchical porous structure and heteroatom doping effects, which combine electrical double-layer capacitors and Faradaic contributions. Our protocol demonstrates a new approach for the potentially eco-friendly benign re-use of sewage sludge and provides a proven technique for synthesizing electrode materials as promising candidates for electrochemical energy storage.

35 **TOC Art**

36

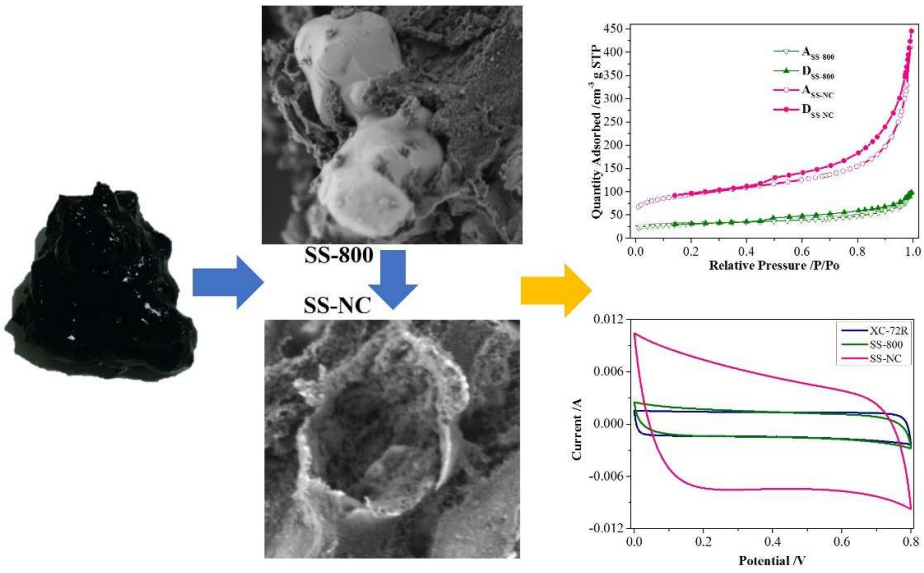

37

38

1. Introduction

Sewage sludge, which is the residue generated from the activated sludge method, consists of organic material, mainly dead bacterial cells and organic pollutants, and inorganic components in the form of silica, iron salts, calcium oxide, alumina, magnesium oxide and a wide variety of transition metals (e.g., Cr, Co and Ni). The European Environmental Agency defines it as "a future waste problem". [1, 2] With the increasing generation of sewage sludge around the world, the disposal of sewage sludge has remained a thorny issue to date.[3] Recently, this issue has been further aggravated by the imposition of more stringent regulations governing the disposal of sewage sludge. Traditional options for sludge disposal such as combustion, landfilling or ocean dumping are no longer acceptable.[4, 5] In this situation, the initiation of more cost-effective, environmentally benign re-use of sewage sludge is certainly necessary from an environmental standpoint.[6, 7]

Sludge pyrolysis, different from sludge combustion, is a proven, innovative technology that can convert approximately half of the organic matter in sewage sludge into useful bioenergy (oil and gas). This process can also immobilize the rest of the organic and inorganic matter into a stabilized form of pyrolytic residue (biochar).[8, 9] Furthermore, sludge pyrolysis is often carried out under inert atmospheric conditions, which precludes the production of highly toxic dioxin-like compounds and particulate matter (e.g., PM2.5). The gases and oils produced in the sludge pyrolysis process can be used as renewable liquid fuels and chemical feedstocks.[10, 11] However, no

value-added utilization has been found for biochar, which is a carbonaceous matrix byproduct that is environmentally resistant.

Supercapacitors are energy storage devices that accumulate energy in the form of electrical charge and bridge the gap between dielectric capacitors and batteries. These devices are attracting considerable attention due to their high specific power, short charging time and long cycle life.[12, 13] Porous carbonaceous materials have been found to be promising candidates for electrical double-layer capacitors (EDLCs) because they possess a large specific area, a more favorable cycle durability and a high level of electrical conductivity.[14, 15] Recently, the synthesis of porous carbonaceous materials derived from waste and biomass for making energy storage materials has attracted considerable attention. For instance, heteroatom-doped porous carbon flakes, porous carbon materials and hierarchically porous carbon nanosheets, which were prepared via carbonization of human hair fibers, broad beans and waste coffee grounds respectively,[16-18] were used for supercapacitor electrode materials, and exhibited high specific capacitance. Compared with conventional carbon precursors (e.g., wood, coal, pitch or nutshell), the cost-effectiveness and environmental friendliness of waste and biomass-derived porous carbon materials make them more suitable for large-scale production and for various practical applications.[16-18] Although biochar produced from sludge pyrolysis holds potential for carbon sequestration, the use of sewage sludge to prepare carbon nanomaterials for EDLCs has not yet been achieved.

In this study, for the first time, we demonstrate the synthesis of

heteroatom-doped carbon materials for EDLCs via the direct pyrolysis of the "all-in-one" precursor sewage sludge. During this pyrolysis process, SiO_2, a special component of sewage sludge, acts as an in-built template that prevents agglomeration and results in the formation of a unique pore size distribution. The organic matter in sewage sludge exhibited as the structure-directing templates through carbonization and graphitizing under the catalytic action of the transition metals. These organic matter abundant in nitrogen and oxygen also serve as the source of heteroatom dopant, which leads to a significant enhancement in the charge storage capacity. The as-synthesized heteroatom-doped carbon material has a high specific surface area, numerous heteroatoms, good electrical transport properties and a meso-/macroporous composite. The electrochemical results demonstrate its favorable charge storage capacity and good stability. The results of our study provide a novel route for the synthesis of heteroatom-doped carbon materials for use in energy storage devices by using a simple, low-cost, green process. This study therefore demonstrates a new approach for the value-added re-use of sewage sludge.

2. Experimental section

2.1. Synthesis of the Sewage Sludge-derived Carbon Material. As the raw material for this process, a dewatered sewage sludge sample was obtained from the Anting wastewater treatment plant in Shanghai, China.[7] The obtained sludge was stored at -20^{o}C before use. All other reagents were of analytical grade and were used as

received unless otherwise stated. All of the water used was prepared with a purification system (Hitech Instrument Co., Shanghai, China).

The sewage sludge-derived heteroatom-doped carbon material was synthesized by a facile one-step pyrolysis process in a quartz tubular reactor (Fig. S1). In brief, the lyophilized sewage sludge was first placed in the quartz tubular reactor under 100 ml/min of N_2 flow for 30 min to remove air. Then the quartz tubular reactor was heated to 800 ^{o}C at a heating rate of 5 ^{o}C/min under a 50 ml/min of N_2 flow, and held at that temperature for 2 h. After being cooled to ambient temperature in the N_2 flow, a resultant black power was obtained and designated as SS-800. The SS-800 was immersed in 20 wt% HF to etch-out the SiO_2, then washed until the pH reached 7, and dried at 100°C. The product of this process was the sewage sludge-derived carbon nanomaterial (SS-NC).

2.2. Characterization. Scanning electron microscopy (SEM; FEI Nova-Nano, The Netherlands) was used to image the morphology of the as-synthesized sewage sludge-derived nanomaterials. The analysis of the surface area, pore diameter and volume was carried out by using the Brunauer-Emmett-Teller (BET) method on an AUTOSORB-IQ instrument (Quantachrome Co., USA). The x-ray diffraction (XRD) patterns were measured with an X' Pert PRO system (Philips Co., The Netherlands) to characterize the crystal structure of the nanomaterials. The functional groups of the as-prepared catalysts were determined by Fourier transform infrared (FTIR) spectra recorded with a VERTEX 70 FT-IR (Bruker Co., Germany) and by Raman analysis with a laser Raman spectrometer (ProTT-RZRaman-B2, Enwave Optronics Inc.,

127 USA). The electronic environment of the nanomaterials was investigated by using
128 X-ray photoelectron spectroscopy (XPS, PHI-5000C, Perkin Elmer Co., USA). The
129 composition of the sewage sludge-derived carbon nanomaterials was measured via
130 energy-dispersive X-ray spectroscopy (EDX) and inductively coupled plasma
131 spectrometry (ICP, Agilent 720ES, USA) after total digestion in a microwave using a
132 mixture of HNO_3 + HCl + HF. The C, O and N contents of the materials were also
133 determined by a Vario EL III Elemental Analyzer (vario EL III, GmbH, Germany).

134 *2.3. Electrochemical Characterization.* All of the electrochemical tests were
135 carried out on a CHI760E electrochemical workstation (Shanghai Chenhua
136 Instruments Co., China) at room temperature in a conventional three-electrode system.
137 An aqueous solution of 0.5 M Na_2SO_4 was used as the electrolyte, a platinum wire
138 was used as the counter electrode and an Ag/AgCl electrode served as the reference
139 electrode. To prepare the work electrode, a slurry containing 80 wt% active material
140 (e.g., SS-800, SS-NC), 10 wt% carbon black (Vulcan XC-72R, surface area 254 m^2/g,
141 Cabot Co., USA) and 10 wt% polytetrafluoroethylene was mixed and loaded on a
142 nickel foam substrate. After being dried in an oven at 353 K for several hours, the
143 as-prepared work electrode was pressed at 15 MPa to assure good electrical contact
144 between the nickel foam substrate and the active material. The electrode was then
145 further dried in an oven at 373 K for several hours. The total mass of the active
146 materials on the nickel foam substrate was about 2~3 mg per electrode with a surface
147 area of 1.0 cm^2.

Cyclic voltammetry (CV) curves were obtained in the potential range of 0-0.8 V vs. Ag/AgCl by varying the scan rate from 5 to 100 mV/s. Electrochemical impedance spectroscopy (EIS) was measured in a frequency range of 10^5 Hz to 0.01 Hz at open circuit voltage with an alternate current amplitude of 5 mV. The EIS results were fitted by ZView software according to the corresponding equivalent circuits. Galvanostatic charge/discharge was carried out at 0.5-8 A/g over a voltage range of 0-0.8 V vs. Ag/AgCl, and the specific capacitance was calculated from the galvanostatic discharge curves according to the following equation (Eq. 1):

$$C = I\Delta t/m\Delta V \quad (1)$$

where C (F/g) is the discharge specific capacitance, I is the discharge current, Δt is the discharge time consumed in the potential range of ΔV and m (g) is the weight of the active materials loaded on the work electrode.

3. Results and discussion

3.1. Textural Properties of the As-synthesized Nanomaterials. The surface morphology and structure of the as-synthesized sewage sludge-derived nanomaterials were examined using SEM, and the typical images are shown in Figure 1. Numerous particles with diameters ranging from about 20 nm to 2 um were identified by EDX as being composed of SiO_2, a special component of sewage sludge. These particles, inlaid into the nanomaterials derived from the sewage sludge (Figs. 1A and B), acted as the in-built template during the synthesized process. This template prevented

agglomeration and resulted in the formation of mesoporous structures combined with graphitization or evaporated of the organic matters in sewage sludge during the pyrolysis process (Figs. 1A and B). The highly porous structures around the SiO_2 particles (Fig. 1B) were formed by the partial graphitization of the organic matter as the carbon precursor.[19] After being immersed in HF, all of these SiO_2 particles vanished. Also, the rough mesoporous structures displayed accumulations of numerous particles with nanometer-sized diameters that increased the surface area of the catalyst (Figs. 1C and D). This accumulation was made further evident by the increased BET surface area of the as-synthesized nanomaterial SS-NC compared with that of the SS-800 (Table 1).

The surface area and pore structure of the as-synthesized sewage sludge-derived nanomaterials were analyzed by the nitrogen adsorption-desorption method. The representative results for SS-800 and SS-NC (Fig. 2A) showed characteristic type IV curves (according to the IUPAC classification) with sharp capillary condensation steps that are typical features of mesoporous solids.[20] The isotherms of the SS-800 and SS-NC all had a clear upward trend at a low relative pressure ($P/P_o < 0.4$), suggesting that the as-synthesized nanomaterials were rich in micropores. The appearance of a sharp upward-type H3 hysteresis loop at $P/P_o > 0.4$ implied the presence of abundant mesopores in the nanomaterials[16, 21]. At high relative pressures before 1.0, the curve exhibited a slight upward tendency, which could be ascribed to the internal macropores that represented the accumulation of particles present in the nanomaterials.

The pore size distributions further suggested the intrinsic hierarchical porous structure of the as-synthesized nanomaterials (Fig. 2B). The peaks observed at 4 nm could be interpreted as mesopores generated by the graphitization or evaporation of organic matters in the sewage sludge. Compared with the SS-800, the increased broad peak observed between 5 and 100 nm for the SS-NC may have corresponded to the mesopores and macropores generated by the removal of SiO_2. The BET surface areas of the nanomaterials significantly increased from 107.44 to 331.39 m^2/g with the etch-out of the in-built SiO_2 template. This increase was accompanied with an expansion of the average pore size from 8.06 to 11.88 nm due to the generated mesopores and macropores. This higher surface area of the SS-NC is advantageous for charge storage.[16, 21]

3.2. Structural Characterization of the As-synthesized Nanomaterials. XRD was used to investigate the phase structure of the as-synthesized sewage sludge-derived nanomaterials (Fig. 2C). Obvious diffraction peaks at 2θ = 20.9° and 26.7° were observed for the SS-800. These peaks corresponded to the typical crystallite structures of SiO_2 (JCPDS, File No. 33-1161) that originate from sewage sludge. However, such peaks disappeared in the SS-NC, indicating the total removal of the hard template. This development was further confirmed by the disappearance of the characteristic asymmetric stretching vibrations of the Si-O-Si (1036 cm^{-1}) peak in the FTIR (Fig. S2A) and the elemental composition of the nanomaterials (Table 1). The HF wishing process could remove most of the unwanted elements. No Si content was detected for

the SS-NC, and this disappearance of Si was accompanied by an increase in the C content from 31.13% to 51.14%.

The amount of Fe content in the sewage sludge and in the as-synthesized nanomaterials was significant, while the content of other heavy metals was relatively low (Fig. S2 and Table 1). The presence of heavy metals such as Fe and Cr would tend to improve the degree of graphitization.[19] A well-developed peak at 22.3° and a weak peak at 43.8°, which corresponded to the (002) and (100) spacing of the graphene stacks, respectively,[16] could be clearly observed. The pattern of the SS-NC also showed several peaks at 15.4°, 29.5°, 30.9 °, 39.2°, 47.1° and 51.5°, which could be attributed to the pentlandite (JCPDS, File No. 08-0090) (Fig. 2C). This pattern suggested the existence of iron sulphide, which is also a type of energy-storage material and may have contributed to the excellent electrochemical performance.[22] It should be noted that there was still some N and O content detected (Table 1), which would suggest that the as-synthesized nanomaterials were N- and O-doped.

FTIR and Raman spectra were used to characterize the structures of the as-synthesized nanomaterial surfaces (Fig. S3). Comparing the FTIR spectra of SS-800 and SS-NC, it could be clearly seen that the characteristic peaks of carbon nanomaterial ranging from 1250 to 1750 cm^{-1} appeared on both curves. These peaks indicated that the framework structures and functional groups were analogous to each other (Fig. S2A).[23] The two peaks in the Raman spectra at around 1335 and 1532 cm^{-1} were the characteristic D and G bands of carbon, which reflected the degree of

disorder and the level of graphitization in the carbon materials, respectively (Fig. S2B).[16, 18, 23] These measurements suggested that the obvious G peak, which accorded with the XRD results, was formed by the partial graphitization of the organic materials as carbon precursors under the catalytic action of the critical toxic heavy metals (e.g., Fe, Cr, Co and Ni) that were uniformly distributed in the sewage sludge. The relatively higher D peak implied defects from the ideal graphitic lattice, which might have been caused by the heteroatom doping effects. The significantly decreased numbers of peaks in the SS-NC compared with those in the SS-800 indicated the removal of impurities, e.g., inorganic matter, accompanied with the etching-out of the in-built SiO_2 template. This process would tend to generate considerable quantities of porous structures, increase the surface areas of the as-synthesized nanomaterials and expose the functional groups in the carbon wall to the pore surfaces.

XPS analysis was used to further analyze the content and chemical state of the elements in the as-synthesized nanomaterials (Fig. 3A). The binding energies were calibrated with respect to the C 1s peak at 284.6 eV. Obvious C 1s and O 1s peaks and fine N 1s, Fe 2p and S 2p peaks were all observed as expected. Compared with SS-800, the intensity ratio of Si 2p vanished, demonstrating the etch-out of the in-built SiO_2 template in accordance with the above-described results. As the positions of the elemental peaks depended on the local chemical environment, high resolution scans of C, O and N were performed and deconvoluted to obtain the corresponding atom binding states by searching for the optimal combination of

Gaussian bands (Figs. 3B, C and D). In the case of the C1s XPS spectrum of SS-NC, the four peaks at 282.8, 284.4, 286.0 and 288.4 eV were attributable to the C-O, C=C, C-C/N and C=O species, respectively (Fig. 3B).[24] The three components of the O1s XPS spectrum, with their peaks at binding energies of about 530.7, 532.1 and 534.6 eV, corresponded to the C=O, C-O and O=C-O species, respectively (Fig. 3C). These components indicated the existence of some oxygen-enriched functionalities in the carbon frameworks. Such oxygen-enriched functionalities have been reported to improve wettability and to produce pseudocapacitance, resulting in better supercapacitive performance. [24]

Sewage sludge contains essential proteins that are abundant in nitrogen. The high-resolution N 1s peaks of SS-NC fit into four types of nitrogen-containing groups at about 398.0, 399.7, 400.8 and 402.5 eV (Fig. 3D). The two peaks located at about 398.0 and 399.7 eV were attributed to pyridinic N and pyrrolic N species, which were assumed to have contributed to the pseudocapacitance. The peak located at 400.8 eV was attributed to quaternary N, which could enhance the electrical conductivity of SS-NC.[25, 26] These results further indicated that N atoms had been successfully doped into the carbonaceous nanomaterials. The introduction of nitrogen into the carbonaceous nanomaterials may have imposed nitrogen-related Faradaic reactions in the electrodes and changed the electron distribution of the materials, thus increasing their supercapacitor performance and enhancing the wettability between the electrode materials and electrolytes.

3.3. Electrochemical Performance of the As-synthesized Nanomaterials as Supercapacitor Electrodes. Electrochemical tests were performed to explore the potential applications of the as-synthesized nanomaterials as electrode materials for EDLCs. The CV curves of XC-72R, SS-800 and SS-NC in 0.5 M Na_2SO_4 aqueous solution at a scan rate of 50 mV/s are shown in Fig. 4A. The control XC-72R exhibited regular rectangular-shaped CV curves, indicating an ideal EDLC nature of the charge-discharge process. The approximately rectangular-shaped and symmetric CV curves of the SS-800 and SS-NC also indicated a dominant contribution of the capacitance from the EDLC. The gravimetric capacitance of the control XC-72R (as calculated from its CV curve with a potential scan rate of 50 mV/s) was 21.29 F/g, which was very close to the values reported in the literature[27] and the 22.03 F/g exhibit by the SS-800. The SS-NC exhibited a much higher specific capacitance of 120.98 F/g. The significant increase of capacitance was mainly attributed to the etch-out of the in-built SiO_2 template, which would not only increase the specific surface area of the nanomaterials but also increase the content of C and the heteroatoms, thereby promoting conductivity and wettability (Table 1).[25, 26] A Faradaic hump was observed at ~0.10 V in the CV curve at low scan rate of 5 mV/s (Fig. 4B), which was probably due to redox reactions of the doped heteroatoms such as pyridinic N and pyrrolic N species, the oxygenated functional groups on the carbon frameworks, or the remaining Fe compounds.[25, 26] As the scan rate increased, the plateau current increased accordingly. The specific capacitance of the SS-NC was up to 178.32 F/g at a potential scan rate of 5 mV/s, which was comparable to the

capacitance of many other EDLCs reported previously.[16-18] The quasi-rectangular shape of the CV curve could still be maintained with little distortion even when the scan rate rose to 100 mV/s (Fig. 4B), which indicated that rapid ion transport and good rate capability could operate in the SS-NC. The distortion of the CV curve reflected the universal characteristic that ion diffusion and transport on the EDLC electrode surface are restricted at high scan rates.

Galvanostatic charge/discharge experiments were carried out at different current densities to further explore the capacitance performance and estimate the specific capacitance of the SS-NC. The appearance of shapes that were almost isosceles triangles demonstrated the ideal charge and discharge characteristics for EDLCs with low dynamic voltage drops and almost 100% Coulombic efficiency over a large voltage range.[18, 26] The insignificant dynamic voltage drop indicated a low internal series resistance, which could also be demonstrated by the EIS (Fig. 5A). The SS-NC had a specific capacitance of 109.73 F/g at a current density of 0.5 A/g (Fig. 4D), which was marginally higher than the previous reports for 100% carbon nanotube (CNT) film (24 F/g) or pristine CNT paper (32 F/g).[18] The 55.26% decrease of the capacitance with a current density increase from 0.5 to 8.0 A/g was attributed to the insufficient electrolyte ion diffusion kinetics at higher operating current densities. These diffusion kinetics would reduce the amounts of electrolyte ions accumulated onto the electrode interfaces and result in the decrement of specific capacitance.[18, 24]

Nyquist plots of the as-synthesized nanomaterials were measured over the frequency range from 10^5 Hz to 0.01 Hz and simulated by ZView software (Fig. 5A). Unlike the SS-800 plot, the plot of SS-NC featured a vertical line in the low-frequency region, which indicated ideal capacitive behavior. This plot was composed of three distinct parts at different frequency ranges.[16, 18, 24] The real impedance (Z'), which was found at very high frequencies with the imaginary impedance near to zero, was the sum of the ohmic resistances (*Rs*) accounting for the electrolyte and the electrode. The *Rs* of the SS-800 (4.47 Ω) was much higher than that of the SS-NC (3.53 Ω), which confirmed that the promoted conductivity was due to the increased content of C and the heteroatoms. The semicircular loop observed at high frequencies represented the composite interfacial impedance and the expected pseudocapacitance impedance that were generated from the Faradaic redox reactions of the electrode material due to the content of N and O species in the carbon frameworks.[16, 18] The inclined portion of the curve (of about 45°) at the middle frequency (which ranged from ~175.8 to ~3.8 Hz) was ascribed to the Warburg impedance, which was the level of encountered impedance to the diffusion of ions from the electrolyte to the electrode surface.[16, 24] The short Warburg resistance section indicated the efficient access of the electrolyte ions to the porous carbon framework of the SS-NC electrode with its hierarchical pore structure. The almost vertical line of the Nyquist plot represented the dominance of ideal double-layer charge/discharge behavior by the as-synthesized SS-NC at low frequencies.[18, 24] Furthermore, the as-synthesized SS-NC exhibited a superior capacitance retention

342 performance. A greater than 99% retention of the initial capacitance of SS-NC was
343 observed after 10000 charge/discharge cycles at a current density of 1 A/g, which
344 indicated its excellent cycling stability (Fig. 5B).

345 *3.4. Significance of This Work.* We synthesized a unique heteroatom (N, O)
346 doped porous carbon nanomaterial, SS-NC, via direct pyrolysis of the "all-in-one"
347 precursor sewage sludge. This material exhibited favorable charge storage capacity
348 with excellent stability and durability. The unique qualities of this carbon
349 nanomaterial and its favorable electrochemical performance as a supercapacitor stem
350 from the particular compositions of sewage sludge and the proper utilization of almost
351 all of the content of the sludge in synthesizing this carbon material. The organic
352 matter in sewage sludge, which is mainly composed of carbon, hydrogen, oxygen and
353 nitrogen, worked as an ideal precursor and nature dopant for the synthesis of
354 heteroatom (N, O) doped porous carbon nanomaterials. The doping of nonmetal
355 heteroatoms in the sp^2 carbon framework not only improved the electrical
356 conductivity and the wettability between the electrodes and electrolytes, but also
357 induced additional pseudocapacitance via reversible redox reactions, consequently
358 improving the capacitive performance of the SS-NC as the electrode.[16, 18, 24]

359 The SiO_2 content in sludge was used as the in-built template. The critical toxic
360 heavy metals (e.g., Fe, Cr, Co and Ni) that are uniformly distributed in sewage sludge
361 with different phases were used as the "in-built catalysts" to catalyze the partial
362 graphitization of the numerous special components of organic matter as carbon
363 precursors during the pyrolyzation process.[19] The intrinsic hierarchical pore

structures of the SS-NC were formed due to the combined effects of the in-built SiO_2 template that prevented agglomeration and the uniformly in-built heavy metal catalysts that produced graphitized areas with a three-dimensional stacking order, resulting in transition-metal-containing carbon materials with essentially highly porous during the pyrolyzation process.[19, 28] These hierarchical pore structures with their unique designs could offer abundant mesopore and macropore structures that could improve the migration and diffusion of the electrolyte ions, resulting in a decreased diffusion distance and high power performance.[29] The micropores within the walls of the mesopores and macropores could supply a highly effective specific surface area for double-layer capacitance to obtain a high specific capacitance and a favorable electrochemical energy storage performance.

The generation of sewage sludge around the world is continually increasing and now exceeds annual totals of 30 million tons in China, 10 million dry tons in the EU and 5.6-7 million dry tons in the US, respectively.[2, 5, 7] In this situation, the need to develop a more cost-effective and environmentally benign value-added re-use of sewage sludge is of particular concern. Our protocol uses the proven pyrolysis technique to convert sewage sludge into a unique porous carbon nanomaterial for the sustainable development of low-cost energy storage devices. This simple and easy-to-handle process is suitable for large-scale industrial production. We suggest that our approach deserves particular attention not only as an eco-friendly and value-added way of re-using sewage sludge, but also as a means of easy fabrication of a low-cost heteroatom-doped nanocarbon composite with a favorable charge storage

386 capacity. The sludge source and property, especially the C content, do has important
387 influence on this preparation. Thus dewatered sewage sludge from domestic
388 wastewater treatment plant is more approach.

389 Although the specific capacitance of the as-synthesis SS-NC is intermediate in
390 all of the reported carbon materials,[16-18, 30] the excellent stability and durability of
391 these materials makes them promising candidates for energy storage devices in many
392 electronics products. Further studies are needed to investigate possible methods of
393 chemical activation (KOH activation and carbonized in NH_3 flow for instance),[16]
394 which are expected to enable additional increases in the specific capacitance of the
395 sewage sludge-derived carbon material by increase its specific surface areas and the N
396 content.

397

398 **4. Conclusions**

399

400 In summary, a unique heteroatom (N, O) doped porous carbon nanomaterial, SS-NC,
401 was synthesized via the direct pyrolysis of sewage sludge, with SiO_2 used as the
402 in-built template, transition metals, the critical toxic components of sewage sludge,
403 used as the graphitizing catalysts, and organic matter, which is mainly composed of
404 carbon, hydrogen, oxygen and nitrogen, worked as an ideal precursor and nature
405 dopant. The SS-NC exhibited favorable charge storage capacity, with a specific
406 capacitance of 109.73 F/g in 0.5 M Na_2SO_4 at a current density of 0.5 A/g, and
407 excellent stability and durability over 10000 charge/discharge cycles. This high

supercapacitor performance can be attributed to the hierarchical porous structure, which provides a highly effective specific surface area for double-layer capacitance, and to the heteroatom doping effects that induce additional pseudocapacitance via a reversible redox reaction. Our protocol shows attractive prospects for establishing an eco-friendly, value-added re-use of sewage sludge. At the same time, our protocol demonstrates a proven technique for synthesizing alternative electrode materials for electrochemical energy storage.

Acknowledgements

The authors wish to thank the National Natural Science Foundation of China (51308401) and the the National Key Technologies R&D Program of China (2014BAC29B01) for their partial support of this study.

References

1 A Plain English Guide to the EPA Part 503 Biosolids Rule. U.S. Envtl. Protection Agency 1994.

2 A. Kelessidis, A. S. Stasinakis, Comparative study of the methods used for treatment and final disposal of sewage sludge in European countries, Waste Manag. 32 (2012) 1186-1195,

3 E. Viau, K. Bibby, T. Paez-Rubio, J. Peccia, Toward a consensus view on the infectious risks associated with land application of sewage sludge, Environ. Sci.

Technol. 45 (2011) 5459-5469,

4 G. Ahlberg, O. Gustafsson, P. Wedel, Leaching of metals from sewage sludge during one year and their relationship to particle size, Environ. Pollut. 144 (2006) 545-553,

5 K. McClellan, R. U. Halden, Pharmaceuticals and personal care products in archived U.S. biosolids from the 2001 EPA national sewage sludge survey, Water Res. 44 (2010) 658-668,

6 K. M. Smith, G. D. Fowler, S. Pullket, N. J. D. Graham, Sewage sludge-based adsorbents: A review of their production, properties and use in water treatment applications, Water Res. 43 (2009) 2569-2594,

7 N. N. Duan, B. Dong, B. Wu, X. H. Dai, High-solid anaerobic digestion of sewage sludge under mesophilic conditions: feasibility study, Bioresour. Technol. 104 (2012) 150-156,

8 N. Takeda, M. Hiraoka, Combined process of pyrolysis and combustion for sludge disposal, Environ. Sci. Technol. 10 (1976) 1147-1150,

9 H. S. Ding, H. Jiang, Self-heating co-pyrolysis of excessive activated sludge with waste biomass: Energy balance and sludge reduction, Bioresour. Technol. 133 (2013) 16-22,

10 A. Domínguez, J. Menéndez, M. Inguanzo, J. Pis, Investigation on the evolution of N-containing organic compounds during pyrolysis of sewage sludge, Biores.Technol. 97 (2006) 1185-1193,

11 A. Domínguez, Y. Fernández, B. Fidalgo, J. Pis, J. Menéndez, Bio-syngas

452 production with low concentrations of CO_2 and CH_4 from microwave-induced
453 pyrolysis of wet and dried sewage sludge, Chemosphere, 70 (2008) 397-403,
454 12 Y. B. He, G. R. Li, Z. L. Wang, C. Y. Su, Y. X. Tong, Single-crystal ZnO
455 nanorod/amorphous and nanoporous metal oxide shell composites: Controllable
456 electrochemical synthesis and enhanced supercapacitor performances, Energy
457 Environ. Sci. 4 (2011) 1288-1292.
458 13 Z. Niu, H. Dong, B. Zhu, J. Li, H. H. Hng, W. Zhou, X. Chen, S. Xie, Highly
459 stretchable, integrated supercapacitors based on single-walled carbon nanotube
460 films with continuous reticulate architecture, Adv. Mater. 25 (2013) 1058-1064
461 14 C. Merlet, B. Rotenberg, P. A. Madden, P. L. Taberna, P. Simon, Y. Gogotsi, M.
462 Salanne, On the molecular origin of supercapacitance in nanoporous carbon
463 electrodes, Nat. Mater. 11 (2012) 306-310
464 15 Y. Zhu, S. Murali, M. D. Stoller, K. J. Ganesh, W. Cai, P. J. Ferreira, A. Pirkle, R.
465 M. Wallace, K. A. Cychosz, M. Thommes, D. Su, E. A. Stach, R. S. Ruoff,
466 Carbon-based supercapacitors produced by activation of graphene, Science 332
467 (2011) 1537-1541
468 16 W. J. Qian, F. X. Sun, Y. H. Xu, L. H. Qiu, C. H. Liu, S. D. Wang, F. Yan, Human
469 hair-derived carbon flakes for electrochemical supercapacitors, Energy Environ.
470 Sci. 7 (2014) 379-386.
471 17 G. Y. Xu, J. P. Han, B. Ding, P. Nie, J. Pan, H. Dou, H. S. Li, X. G. Zhang,
472 Biomass-derived porous carbon materials with sulfur and nitrogen dual-doping
473 for energy storage, Green Chem. 17 (2015) 1668-1674.

474 18 Y. S. Yun, M. H. Park, S. J. Hong, M. E. Lee, Y. W. Park, H. J. Jin,
475 Hierarchically porous carbon nanosheets from waste coffee grounds for
476 supercapacitors, ACS Appl. Mater. Interfaces 7 (2015) 3684-3690.
477 19 F. J. Maldonado-Hódar, C. Moreno-Castilla, J. Rivera-Utrilla, Y. Hanzawa, Y.
478 Yamada, Catalytic graphitization of carbon aerogels by transition
479 metals, Langmuir 16 (2000) 4367-4373.
480 20 X. F. Qian, B. Li, Y. Y. Hu, G. X. Niu, D. Y. H. Zhang, R. C. Che, Y. Tang, D. S.
481 Su, A. M. Asiri, D. Y. Zhao, Exploring meso-/microporous composite molecular
482 sieves with core-shell structures, Chem. Eur. J. 18 (2012) 931-939.
483 21 S. Kondrat, C. R. Perez, V. Presser, Y. Gogotsi, A. A. Kornyshev, Effect of pore
484 size and its dispersity on the energy storage in nanoporous
485 supercapacitors, Energy Environ. Sci. 5 (2012) 6474-6479.
486 22 J. Q. Yang, X. C. Duan, Q. Qin, W. J. Zheng, Solvothermal synthesis of
487 hierarchical flower-like b-NiS with excellent electrochemical performance for
488 supercapacitors, J. Mater. Chem. A 1 (2013) 7880-7884.
489 23 S. Y. Zhao, J. Liu, C. X. Li, W. B. Ji, M. M. Yang, H. Huang, Y. Liu, Z. H. Kang,
490 Tunable ternary (N, P, B)-doped porous nanocarbons and their catalytic
491 properties for oxygen reduction reaction, ACS Appl. Mater. Interfaces 6 (2014)
492 22297-22304.
493 24 J. Zhou, Z. S. Zhang, W. Xing, J. Yu, G. X. Han, W. J. Si, S. P. Zhuo,
494 Nitrogen-doped hierarchical porous carbon materials prepared from

meta-aminophenol formaldehyde resin for supercapacitor with high rate performance, Electrochimica Acta 153 (2015) 68-75.

25 X. Liu, M. Antonietti, Moderating black powder chemistry for the synthesis of doped and highly porous graphene nanoplatelets and their use in electrocatalysis, Adv. Mater. 25 (2013) 6284-6290.

26 Z. Liu, H. G. Nie, Z. Yang, J. Zhang, Z. P. Jin, Y. Q. Lu, Z. B. Xiao, S. M. Huang, Synergistically enhanced activity of graphene quantum dot/multi-walled carbon nanotube composites as metal-free catalysts for oxygen reduction reaction, Nanoscale 5 (2013) 3283-3288.

27 T.A. Centeno, F. Stoeckli, The role of textural characteristics and oxygen-containing surface groups in the supercapacitor performances of activated carbons, Electrochim Acta 52 (2006) 560-566.

28 R. W. Fu, T. F. Baumann, S. Cronin, G. Dresselhaus, M. S. Dresselhaus, J. H. Satcher, Formation of graphitic structures in cobalt-and nickel-doped carbon aerogels, Langmuir 21 (2005) 2647-2651.

29 H. Zhu, X. Wang, X. Liu, X. Yang, Integrated synthesis of poly(o-phenylenediamine)-derived carbon materials for high performance supercapacitors, Adv. Mater. 24 (2012) 6524-6529.

30 M. Biswal, A. Banerjee, M. Deo, S. Ogale, From dead leaves to high energy density supercapacitors, Energy Environ. Sci. 6 (2013) 1249-1259.

516 Table 1. Properties of the as-synthesized sewage sludge-derived catalysts

	SS-800	SS-NC
S_{BET} (m^2/g)	107.44	331.39
average pore size (nm)[a]	8.06	11.88
conc. (wt %)		
C [b]	31.13	51.14
N [b]	0.69	1.28
O [c]	22.40	18.46
Fe [d]	11.87	4.15
Si [d]	6.67	-
Al [d]	0.02	0.03
Mg [d]	0.06	0.40
Ca [d]	0.59	0.87
Cr [d]	0.03	0.02
Mn [d]	0.12	0.03
Ni [d]	0.08	0.04
Cu [d]	0.11	0.11

517 [a]: Calculated from the Barrett-Joyner-Halenda equation using the desorption isotherm.

518 [b]: The contents of C and N were obtained by Elemental Analyze.

519 [c]: The content of O was obtained by EDX.

520 [d]: The contents of Si and metals were obtained by ICP.

521

Figure Legends

Figure 1. Textural properties of the as-synthesized catalysts. SEM images of the as-prepared SS-800 (A, B) and SS-NC (C, D).

Figure 2. N_2 adsorption-desorption isotherms (A), pore size distributions (B) (A represents absorption and D represents desorption) and (C) XRD spectrum (G represents graphene and P represents pentlandite) of the SS-800 and SS-NC.

Figure 3. X-ray photoelectron spectra of the as-synthesized SS-800 and SS-NC (A). The high resolution C1s, O1s and N1s XPS spectra of the SS-NC are shown in (B), (C) and (D), respectively.

Figure 4. Electrochemical performance of the as-synthesized nanomaterials as supercapacitor electrodes. (A) CV measurements of XC-72R, SS-800 and SS-NC in 0.5 M Na_2SO_4 aqueous solution over a potential range from 0 to 0.8 V at a scan rate of 50 mv/s. (B) CV measurements of SS-NC at different scan rates. (C) Charge-discharge curves of SS-NC at different current densities. (D) Specific capacitances of SS-NC at different current densities.

Figure 5. (A) Partial enlargement of the Nyquist plot in the high-frequency region with its entire range shown in the inset. (B) Long-term cycling performance of the

544 SS-NC during 10000 charge/discharge cycles at a current density of 1 A/g.

545

546

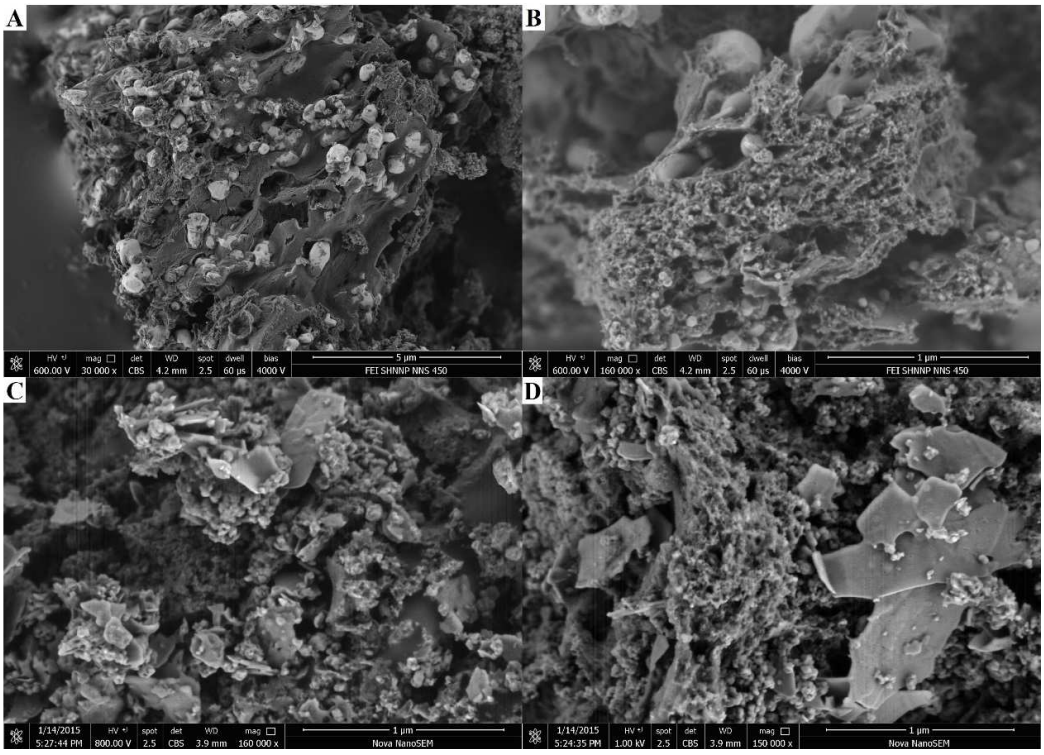

547

548

549

550 **Figure 1.**

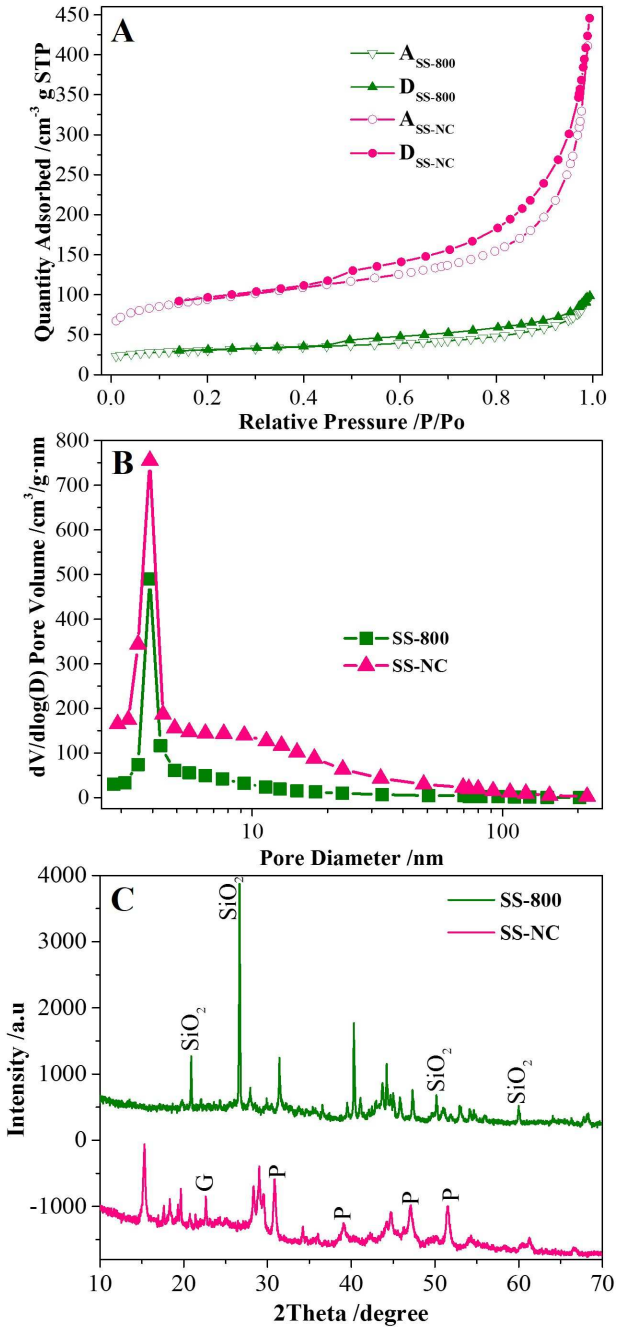

Figure 2.

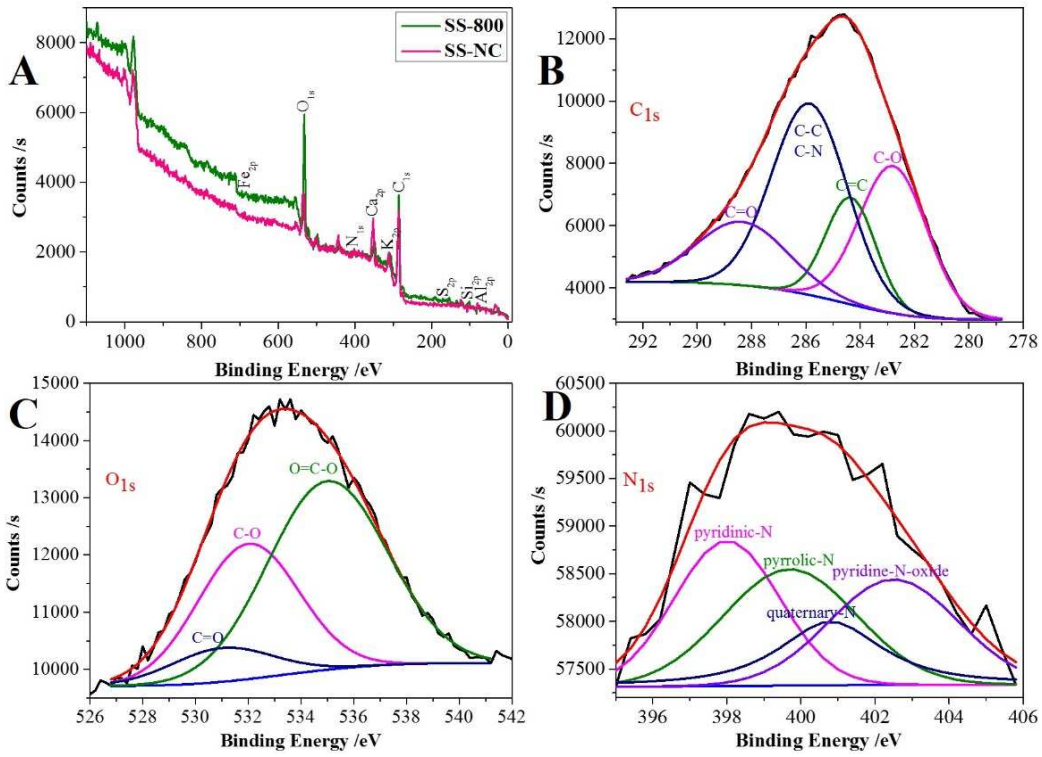

Figure 3.

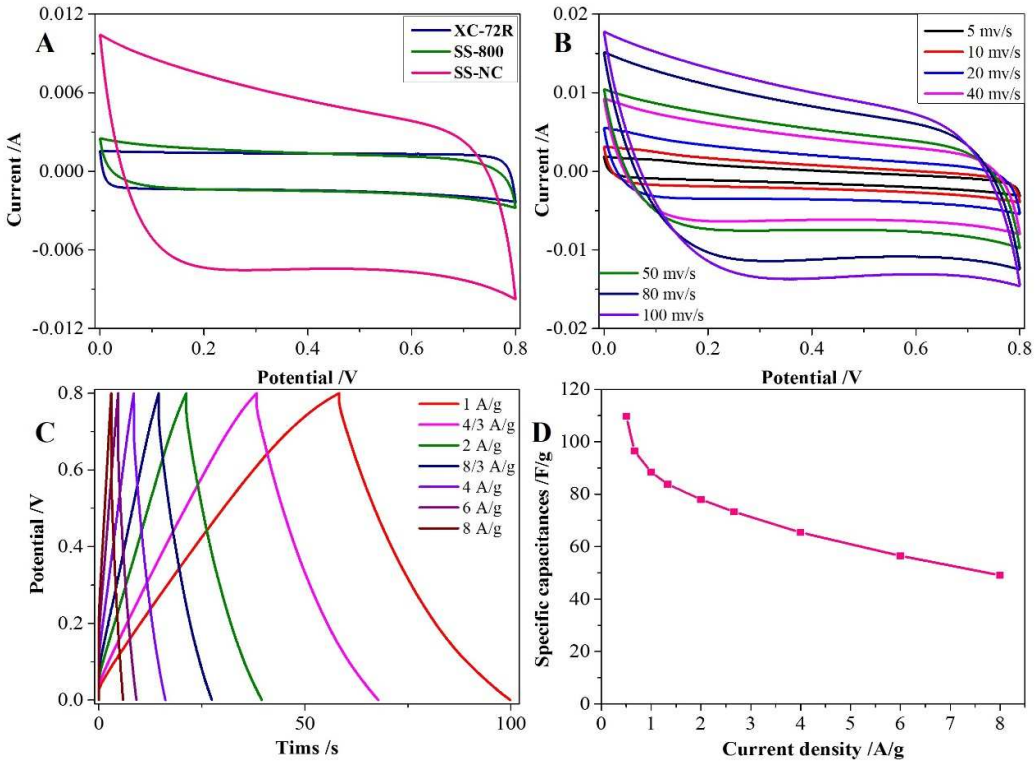

Figure 4.

570

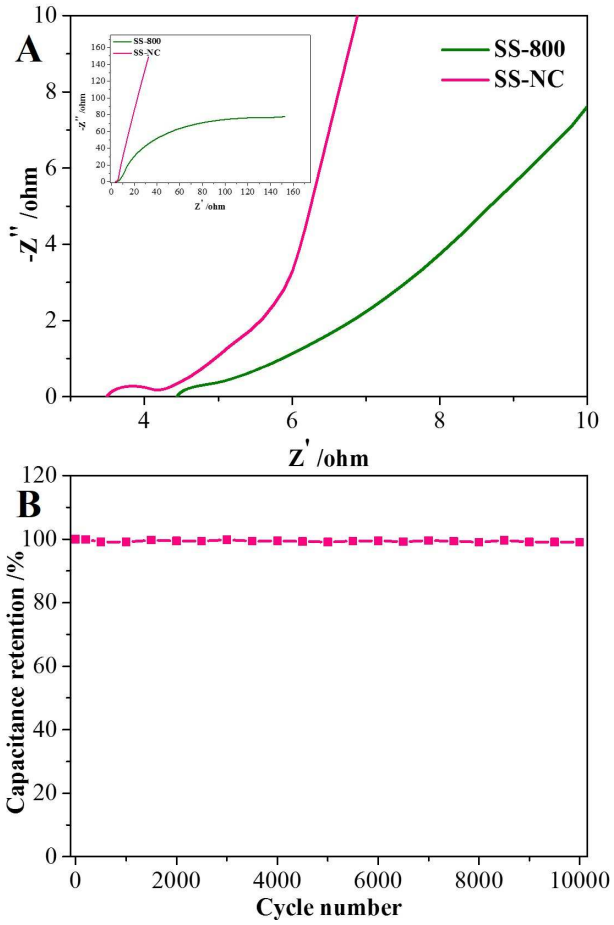

571

572

573

574 **Figure 5.**

Graphical contents entry

A unique heteroatom (N, O) doped porous carbon nanomaterial with favorable charge storage capacity and excellent stability and durability was synthesized via direct pyrolysis of the "all-in-one" precursor sewage sludge.